

# Seasonality of phytoplankton growth limitation by iron and manganese in subantarctic waters

Pauline Latour<sup>1</sup>, Robert F. Strzepek<sup>2</sup>, Kathrin Wuttig<sup>3</sup>, Pier van der Merwe<sup>4</sup>, Sam Eggins<sup>5</sup>, Lennart T. Bach<sup>1</sup>, Philip W. Boyd<sup>1</sup>, Michael J. Ellwood<sup>5</sup>, Terry L. Pinfeld<sup>6</sup>, and Andrew R. Bowie<sup>1</sup>

<sup>1</sup>Institute for Marine and Antarctic Studies, University of Tasmania

<sup>2</sup>Antarctic Climate and Ecosystems Cooperative Research Centre (ACE CRC), University of Tasmania

<sup>3</sup>Antarctic Climate and Ecosystems Cooperative Research Centre (ACE CRC), University of Tasmania

<sup>4</sup>Australian Antarctic Program Partnership (AAPP), Institute for Marine and Antarctic Studies, University of Tasmania

<sup>5</sup>Research School of Earth Sciences, Australian National University

<sup>6</sup>School of Medicine, College of Health and Medicine, University of Tasmania

November 26, 2022

## Abstract

Phytoplankton indirectly influence the climate, through their role in the ocean biological carbon pump. Hence factors limiting phytoplankton growth directly impact the strength of the biological carbon pump and consequently climate. In the Southern Ocean, the subantarctic zone represents an important carbon sink, yet variables limiting phytoplankton growth are not fully constrained. Co-limitation by iron (Fe) and manganese (Mn) has recently been observed in the coastal and offshore Southern Ocean, but very few studies have focused on the subantarctic zone. In addition, no study has investigated the seasonal variability of Mn (co-)limitation of phytoplankton growth in the Southern Ocean. Using three shipboard bioassay experiments, we evaluated the seasonality of Fe and Mn co-limitation of subantarctic phytoplankton growth, south of Tasmania. We observed a strong seasonal variation in phytoplankton Fe limitation, and that the response of phytoplankton to Mn was subtle and thus readily masked by the responses to Fe. Combined addition of Fe and Mn enhanced carbon uptake of nanoeukaryotes in spring and microeukaryotes in summer while the addition of Mn alone stimulated the growth of picocyanobacteria in autumn. These results suggest the importance of Mn may vary seasonally and its control on phytoplankton growth may be associated with specific taxa.



39 picocyanobacteria in autumn. These results suggest the importance of Mn may vary seasonally and its  
40 control on phytoplankton growth may be associated with specific taxa.

## 41 Introduction

42 Phytoplankton play a major role in the marine carbon cycle by driving the transfer of carbon dioxide  
43 from the atmosphere into the ocean through photosynthesis. This process is part of the biological carbon  
44 pump, and its strength varies between and within oceanic regions (Lenton et al. 2013; Deppeler and  
45 Davidson 2017). The Southern Ocean is comprised of several biogeochemical regions with contrasting  
46 hydrographic and nutrient conditions: the subantarctic zone, the polar front zone, the Antarctic zone,  
47 and the seasonal sea ice zone, each delimited by fronts (Orsi et al. 1995). South of the subtropical front,  
48 phytoplankton growth is mainly limited by very low concentrations of iron (Fe) (Boyd et al. 2000;  
49 Deppeler and Davidson 2017). Other factors may also limit phytoplankton growth, such as low light  
50 and temperature, or specifically north of the polar front, low silicic acid levels (Boyd 2002; Bowie et  
51 al. 2009; Strzepek et al. 2012). These limiting factors (alone or combined) directly impact the strength  
52 of regional biological carbon pump and hence need to be identified to project changes to the oceanic  
53 carbon cycle during the Anthropocene.

54 Interest in nutrient co-limitation of Southern Ocean phytoplankton has recently grown (Middag et al.  
55 2013; Browning et al. 2014; Browning et al. 2021). Specifically, several studies have identified Fe and  
56 manganese (Mn) co-limitation in both coastal (Wu et al. 2019) and open ocean waters (Browning et al.  
57 2021) of the Southern Ocean. Co-limitation occurs when two or more elements limit phytoplankton  
58 growth simultaneously, and several kinds of co-limitation have been identified. Saito et al. (2008)  
59 classified Mn co-limitation as a type II “Biochemical substitution co-limitation”, in which two elements  
60 are expected to substitute for each other for the same active site of an enzyme, for example, Fe and Mn  
61 within the superoxide dismutase enzyme. Manganese is an essential element for phytoplankton growth,  
62 used in the oxygen-evolving complex for the water-splitting reaction of photosynthesis and in the  
63 superoxide dismutase enzyme to defend against reactive oxygen species (ROS) (Sunda et al. 1983;  
64 Peers and Price 2004). Therefore, phytoplankton growth may be limited in regions where dissolved Mn  
65 (dMn) concentrations are particularly low, such as the Southern Ocean (Westerlund and Öhman 1991;  
66 Middag et al. 2011, 2013; Latour et al. 2021). Importantly, phytoplankton Mn requirements may vary  
67 depending on Fe conditions. Peers and Price (2004) observed that diatoms increased their Mn content  
68 under Fe stress, presumably to produce more superoxide dismutase enzyme to counter the additional  
69 ROS production associated with Fe limitation. If Fe limitation increases the cellular requirement for  
70 Mn, Mn (co-)limitation may be expected in Southern Ocean phytoplankton limited by Fe (Boyd et al.  
71 2000; Deppeler and Davidson 2017). However, several earlier shipboard incubation experiments in  
72 Southern Ocean waters did not observe an effect of Mn addition in either coastal or open waters of the  
73 Southern Ocean during the austral spring and summer (Buma et al. 1991; Scharek et al. 1997; Sedwick

74 et al. 2000), suggesting that Mn (co-)limitation is not pervasive within the Southern Ocean and may  
75 vary between regions and seasons.

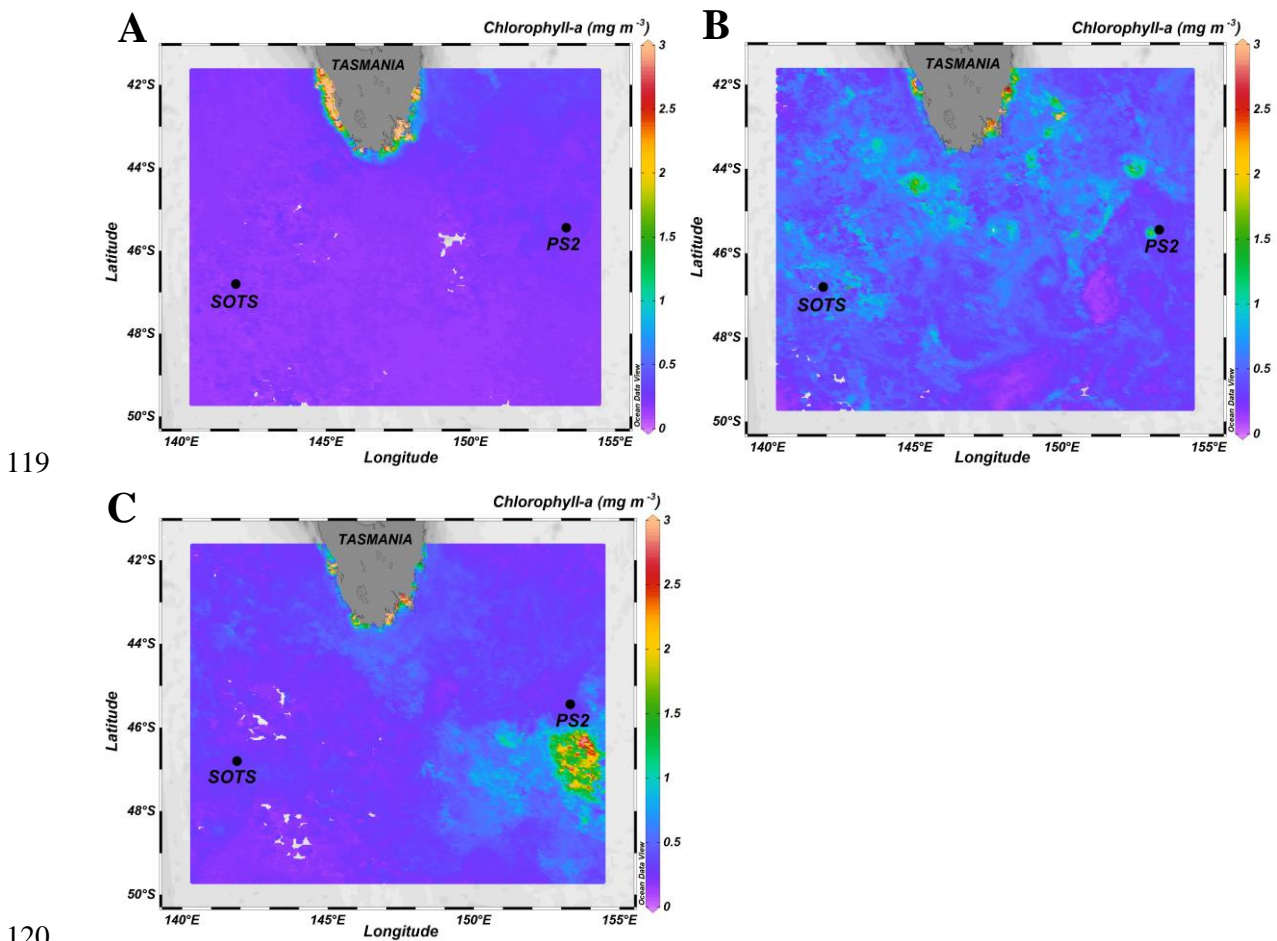
76 The subantarctic zone, the northernmost region of the Southern Ocean, sustains the strongest carbon  
77 uptake of all the Southern Ocean biogeochemical regions (Lenton et al. 2013). In terms of biology, this  
78 region sees the transition from phytoplankton communities containing coccolithophores and fewer  
79 diatoms in northern waters towards more diatoms and less coccolithophores in polar waters (Trull et al.  
80 2001). Usually, pico- and nanoplankton dominate phytoplankton communities in terms of cell counts,  
81 but high grazing pressure keeps their abundance relatively low with little seasonal variability (Deppeler  
82 and Davidson 2017 and references therein). In this region, Fe was demonstrated as the main factor  
83 limiting phytoplankton growth, with silicic acid possibly (co-)limiting diatoms (Boyd et al. 1999;  
84 Westwood et al. 2011; Eriksen et al. 2018). Until now, the study of Fe-Mn co-limitation of  
85 phytoplankton growth has been restricted to a few polar Southern Ocean sites (Buma et al. 1991;  
86 Scharek et al. 1997; Sedwick et al. 2000; Wu et al. 2019; Browning et al. 2021), with only the Browning  
87 et al. (2021) study looking at potential co-limitation within subantarctic waters. A recent study showed  
88 that dMn concentrations are low in subantarctic waters south of Tasmania, with an average  
89 concentration of 0.24 nM measured within the surface mixed layer during the austral summer 2018  
90 (Latour et al., 2021). In this region, Mn, like Fe, may be delivered to the ocean through atmospheric  
91 inputs from Tasmania and mainland Australia or sedimentary inputs from the Tasmanian shelf.  
92 Southward advection of subtropical waters has also been observed to supply Fe and Mn enriched waters  
93 to the subantarctic zone (Sedwick et al. 2008; Bowie et al. 2009; Latour et al. 2021). To date, no studies  
94 have investigated Fe and Mn co-limitation in the Australian sector of the Southern Ocean. Additionally,  
95 to our knowledge, there has been no prior study of the seasonality of Mn or Fe-Mn (co-)limitation in  
96 any subantarctic region.

97 This study presents the results of three shipboard incubation experiments performed in subantarctic  
98 waters in the Australian sector of the Southern Ocean examining Fe-Mn co-limitation in austral spring,  
99 summer, and autumn. We expect that following wind-mixing in winter, both dissolved Fe (dFe) and  
100 dMn levels should be higher in surface waters during spring due to supply from deeper  
101 waters/subsurface maxima and external sources (e.g. about 0.3-0.4 nM for dFe and dMn; Bowie et al.  
102 2009; Latour et al. 2021). Therefore, we hypothesize Fe and Mn will not (co-)limit phytoplankton  
103 growth in spring. In summer, dFe and dMn should decrease due to biological uptake and reduced  
104 vertical nutrient inputs resulting from stronger stratification. Hence, Fe limitation of phytoplankton  
105 growth will likely occur. Iron stress may increase phytoplankton Mn requirements (Peers and Price  
106 2004), and due to the decrease of dMn concentrations from biological uptake during the spring season,  
107 dMn may (co-)limit phytoplankton growth. In autumn, trace metal levels should be at their lowest,  
108 hence we hypothesize Mn, Fe or both will strongly limit phytoplankton growth, depending on the ratios  
109 of both elements relative to biological demand.

110 **Material and Methods**

111 **SAMPLING**

112 The bioassay experiments were performed onboard the RV *Investigator* during three voyages, IN2018-  
113 V04 (September/October 2018, austral spring), IN2019-V02 (March/April 2019, austral autumn) and  
114 IN2020-V08 (December/January 2020-21, austral summer). The first experiment was conducted at  
115 Process Station 2 (PS2) of the East Australian Current voyage IN2018-V04 (45.44°S, 153.31°E) and  
116 the following two experiments at the Southern Ocean Time Series (SOTS) station (46.80°S, 141.884°E)  
117 (Figure 1). Both sites are within the subantarctic zone to the southeast and southwest of Tasmania,  
118 respectively (Bowie et al. 2011).



121 Figure 1: Sites sampled for each experiment. The background image colour shading represents the monthly  
122 average surface chlorophyll-a concentrations measured by satellite (MODIS-Aqua, 8-day average 4 km) for the  
123 month when each of the bioassay experiments was performed. A: phytoplankton incubations at PS2 during the  
124 spring voyage (IN2018-V04), monthly average for September 2018. B: phytoplankton incubations at SOTS during  
125 the summer voyage (IN2020-V08), monthly average for December 2020. C: phytoplankton incubations at SOTS  
126 during the autumn voyage (IN2019-V02), monthly average for March 2019.

127 Seawater used for the bioassay experiments was collected at 15 m depth for the first two experiments  
128 (spring and autumn) and at 20 m for the summer experiment using a polyurethane powder-coated  
129 aluminium rosette, or “Trace Metal Rosette” (TMR) (Sea-bird Scientific, USA; Holmes et al. 2020).  
130 Samples for macronutrients, flow cytometry and photophysiology analyses were collected from the

131 TMR to characterise the initial phytoplankton communities. Polycarbonate bottles used for the  
132 incubations were washed with Neutracon detergent for 48h, and then in 10% hydrochloric acid (HCl)  
133 for 7 days to remove trace metal contamination. After multiple Milli-Q water rinses, bottles were dried  
134 overnight in an ISO Class 5 laminar flow hood before being double-bagged in plastic. Onboard, the  
135 bottles were rinsed three times with the incubation seawater before filling them inside an ISO Class 5  
136 containerized clean room. The seawater was unamended (Control) or spiked with a solution of Fe, Mn  
137 or a combination of both. The Fe and Mn spikes were prepared in 0.01 M Ultrapure HCl using ultrapure  
138 salts of  $\text{FeCl}_3$  (or  $\text{FeNO}_3$  for the spring experiment) and  $\text{MnCl}_2$ . Triplicates were used for each treatment,  
139 resulting in 12 bottles for 4 treatments, named hereafter: Control, +Fe, +Mn, and +FeMn.  
140 Concentrations of Fe and Mn were adjusted to reach a final concentration of at least 2 nM, which we  
141 considered as nutrient-replete conditions (Browning et al. 2021). The bottles were then incubated in  
142 deck board incubators inside mesh bags to reproduce the light penetrating the surface ocean, at  
143 approximately 15 m (80% of incident irradiance). Deck board incubators allowed the algal communities  
144 to follow their regular diel light:dark cycles. The temperature of the incubators was maintained by a  
145 continuous flow of seawater, keeping the bottles at the same temperature as the surrounding surface (~  
146 7 m) seawater. Sampling was done at day 7 for macronutrients, flow cytometry and photophysiology  
147 analyses for each experiment. Flow cytometry samples were fixed using 2% (v/v) glutaraldehyde  
148 (Electron-microscope grade, 25%), for phytoplankton samples collected during the second voyage in  
149 autumn 2019. For the summer 2020 voyage, a mixture of formaldehyde-hexamine (18%:10% v/w) was  
150 used to preserve phytoplankton samples. Due to a technical issue, flow cytometry samples from the  
151 spring 2018 voyage were lost and are therefore not presented in this study. All bacteria samples were  
152 fixed using 2% glutaraldehyde (Electron-microscope grade, 25%). All flow cytometry samples were  
153 held at 4°C in the dark for 25-30 min after being fixed and were then flash-frozen in liquid nitrogen and  
154 stored in a -80°C freezer until analyses back onshore.

155 Following the subsampling, a portion of the remaining seawater was dispensed into 300 mL acid-  
156 washed polycarbonate bottles and spiked with 16-20  $\mu\text{Ci}$  of Sodium  $^{14}\text{C}$ -bicarbonate ( $\text{NaH}^{14}\text{CO}_3$ ;  
157 specific activity 1.85 GBq  $\text{mmol}^{-1}$ ; PerkinElmer, USA) and 0.2 nM of an acidified  $^{55}\text{Fe}$  solution ( $^{55}\text{FeCl}_3$   
158 in 0.1 M Ultrapure HCl; specific activity 30 MBq  $\text{mmol}^{-1}$ ; PerkinElmer; Ellwood et al. 2020). Bottles  
159 were then incubated in the deck board incubators for another 24 h, under the same conditions as the  
160 bioassay experiments. The spiked samples were then filtered sequentially through 0.2, 2 and 20  $\mu\text{m}$   
161 polycarbonate filters (47 mm diameter; Poretics, USA), separated by 200  $\mu\text{m}$  nylon mesh spacers. The  
162 filters were washed with Titanium(III) EDTA – citrate reagent for 5 min to dissolve Fe (oxy)hydroxides  
163 and remove extracellular particle-bound ferric ions and rinsed three times with 15 mL of 0.2  $\mu\text{m}$ -filtered  
164 seawater. Finally, filters were placed in 20 mL glass vials (Wheaton Industries, USA) and acidified with  
165 200  $\mu\text{L}$  of 1.2 M HCl. These filters were then stored at room temperature for analyses on shore.

166 ANALYSIS

167 Dissolved macronutrients were analysed onboard using segmented flow analysis (Rees et al. 2018). One  
168 silicic acid measurement was removed from the analysis due to an inconsistent result (autumn  
169 experiment, in the “Mn” treatment). In summer, several silicic acid concentrations measured had a value  
170 below the detection limit (0.2  $\mu\text{M}$ ) and were therefore replaced by this same value. Final nitrate  
171 concentrations are not presented due to the use of an  $\text{FeNO}_3$  solution for the Fe spike during the spring  
172 experiment. However, initial nitrate concentrations are mentioned in the discussion. Phosphate and  
173 silicic acid uptake rates were calculated by subtracting the final value measured in each bottle from the  
174 initial concentrations to calculate an average uptake rate per week over the 7-day period of incubation.  
175 Initial dissolved trace metal concentrations were measured through Sector Field Inductively Coupled  
176 Plasma mass spectrometry (SF-ICP-MS) after preconcentration and matrix removal through seaFAST  
177 at the Australian National University (Canberra, Australia). Dissolved Fe and Mn concentrations were  
178 used to estimate Mn deficiency relative to Fe as  $\text{Mn}^* = \text{dMn-dFe}/R_{\text{Fe:Mn}}$ , where  $R_{\text{Fe:Mn}}$  is the average  
179 Fe:Mn ratio of phytoplankton (Moore 2013; Browning et al. 2021). If  $\text{Mn}^* > 0.1$ , this suggests Mn  
180 replete conditions.

181 Fast Repetition Rate Fluorometry (FRRF) was used to determine the maximum photochemical  
182 efficiency ( $F_v/F_m$ ) and functional absorption cross section ( $\sigma_{\text{PSII}}$ ) of photosystem II (PSII) using a Light-  
183 induced Fluorescence Transients Fast Repetition Rate (LIFT-FRR) fluorometer (Soliense, USA). After  
184 low light ( $2 \mu\text{mol photons m}^{-2} \text{s}^{-1}$ ) acclimation for ~30 minutes, samples were exposed to 140 flashes of  
185 light every 2.5  $\mu\text{sec}$  (saturation sequence) to saturate PSII and the first stable electron acceptor,  $Q_A$  after  
186 which the time interval between flashes was increased exponentially (relaxation sequence) for 90  
187 flashes.  $F_v/F_m$  (where  $F_v = F_m - F_o$ ) was calculated from  $F_o$  and  $F_m$ , which refer to the minimum and  
188 maximum fluorescence in the dark-acclimated state, respectively.  $F_v/F_m$  and  $\sigma_{\text{PSII}}$  were determined from  
189 the mean of 200 iterations of the fluorescence induction and relaxation protocol measured at 470 nm.  
190 At least 10 acquisitions were measured for each sample and used to calculate the average value of  $F_v/F_m$   
191 and  $\sigma_{\text{PSII}}$ . Due to recalibration of the instrument between voyages, no direct comparison of the initial  
192 fluorescence ( $F_o$ ) results can be made between seasons, but only between treatments for the same  
193 season.

194 Flow cytometry samples were analysed at Menzies Institute for Medical Research (University of  
195 Tasmania, Hobart), using an Aurora Cytek flow cytometer. This instrument can measure particles  
196 ranging from 200 nm up to at least 60  $\mu\text{m}$ . However, the largest size particles possibly measured by this  
197 instrument has not yet been determined. Briefly, frozen samples were thawed at  $37^\circ\text{C}$  for 5-10 minutes  
198 before running 500  $\mu\text{L}$  of unstained samples at flow rates of ~50  $\mu\text{L}$  per minute, using Milli-Q water as  
199 sheath fluid. Violet and blue excitation lights were used to differentiate main phytoplankton groups  
200 through their fluorescence pigments: chlorophyll with red fluorescence and phycoerythrin with orange  
201 fluorescence, respectively, against forward scatter (FSC). All scatter and fluorescence parameters were

202 analysed based on values from the integrated area of the excitation peak. Results obtained from both  
203 the summer and autumn voyages were analysed using SpectroFlo software. For an overall comparison  
204 between the two seasons, phytoplankton communities were divided into three gates: picoeukaryotes,  
205 nanoeukaryotes and large phytoplankton (microeukaryotes), identified on the violet channel (V12, 405  
206 nm excitation, 692 nM emission) against FSC. If the signal from V12 was saturated, we used another  
207 excitation wavelengths (B7, 488 nm excitation, 661 nM emission). Picocyanobacteria were isolated on  
208 another fluorescence channel (B4, 488 nm excitation, 581 nM emission) due to the presence of  
209 phycoerythrin (Marie et al. 1999). Cell counts per unit volume were determined from the instrument  
210 through the known volume analysed. We then used the cell counts to calculate the relative importance  
211 of each group in terms of population size ( $F_{pop}$  described below) by comparing their size (FSC) and  
212 abundance, using the following equation from Bach et al. (2018):

$$213 \quad F_{pop} = \frac{N_{pop} \times FSC_{pop}}{N_{all} \times FSC_{all}} \quad (1)$$

214 Where F represent the fraction of size (size is here represented by the parameter FSC) produced by a  
215 specific population (pop). N represents an abundance via cell count of a specific population or all  
216 phytoplankton cells (all).

217 Heterotrophic bacterial counts were performed after the addition of SYBR Green I stain (1000-fold  
218 dilution) on thawed fixed samples. Samples were incubated with the stain for 15 minutes at room  
219 temperature in the dark. Then, a 50  $\mu$ L aliquot of stained sample was run on the instrument at high flow  
220 rate. Bacteria were identified using blue excitation and green fluorescence (B2, 488 nm excitation, 525  
221 nM emission). Cell counts were determined as described above for phytoplankton.

222 Iron uptake and net primary productivity (carbon uptake) were determined by measuring disintegrations  
223 per minute (DPM) on a liquid scintillation counter (PerkinElmer Tri-Carb 2910 TR). Filters were  
224 incubated at least 24h prior analysis in 10 mL of Ultima Gold liquid scintillation cocktail (Perkin  
225 Elmer). Daily carbon incorporation rates were estimated following Hoppe et al. (2017). The uptake of  
226  $^{55}\text{Fe}$  and  $^{14}\text{C}$  were corrected for ambient dFe and dissolved inorganic carbon concentrations.

## 227 STATISTICAL TESTS

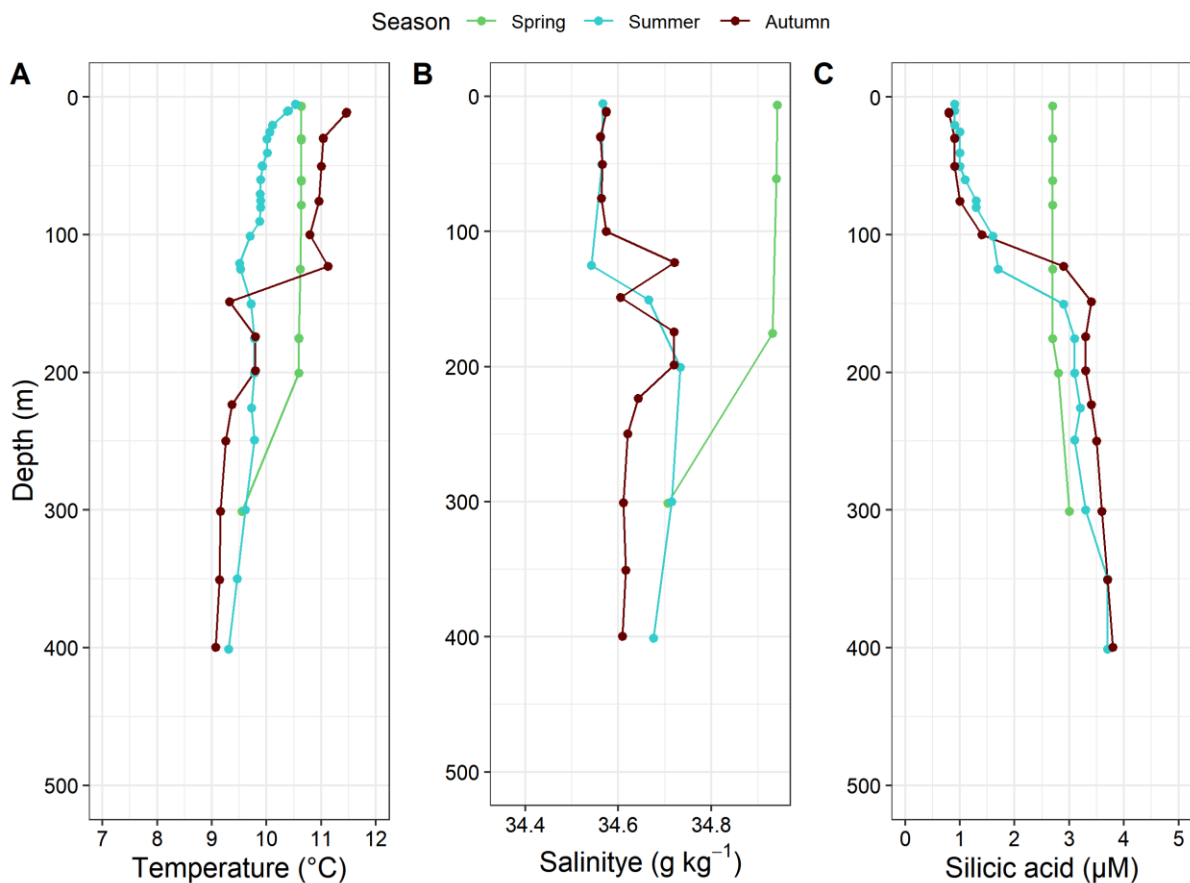
228 Statistical analyses were performed in R (R “stats” package; R Core Team 2020). Datasets were initially  
229 examined for homogeneity of variance using a Levene’s test, and normality using a Shapiro-Wilk.  
230 Where data were both normally distributed and homoscedastic, significant differences between  
231 treatments were investigated using a one-way analysis of variance (ANOVA) with a Tukey’s HSD post  
232 hoc test. Otherwise, a Kruskal-Wallis test was performed followed by a Wilcoxon signed-rank test  
233 where the former result was significant. A p-value of 0.05 was used to identify significant difference  
234 between treatments.

235 During the autumn experiment, no statistical tests could be performed on the Fe uptake results for the  
236 +Fe treatment due to a mistake in the radioisotope additions.

## 237 Results

### 238 INITIAL CONDITIONS

239 Oceanographic conditions differed between the three experiments across temperature, salinity and  
240 silicic acid profiles (Figure 2). In spring, the surface ocean was characterized by a deep mixed layer  
241 depth (MLD), down to 200 m. Temperature, salinity and silicic acid concentrations were constant within  
242 the mixed layer with values at about 10.5°C, 34.9 g kg<sup>-1</sup> and < 3 μM, respectively. In summer, stronger  
243 stratification was observed with the MLD reaching just below 100 m. The surface temperature was like  
244 spring but lower below 25 m (about 10°C). In summer, the salinity was much lower than in spring (<  
245 34.6 g kg<sup>-1</sup>). Similarly, silicic acid concentrations were lower in summer, down to 1 μM in surface  
246 waters. In autumn, the MLD reached 100 m, where the temperature was ≥ 11°C and the salinity was  
247 like summer conditions. Silicic acid concentrations were the lowest, with less than 1 μM in surface  
248 waters.



249

250 Figure 2: Temperature (A), salinity (B) and silicic acid concentrations (C) depth profiles measured at the  
251 experiment sites: PS2 (spring) and SOTS (summer and autumn). Colours represent the seasons: spring in green,  
252 summer in blue and autumn in brown.

253 Initial dFe and dMn concentrations present in the incubated seawater were slightly different between  
 254 seasons (Table 1). The dFe concentration was the highest in summer, with intermediate values measured  
 255 in spring and lowest concentrations in autumn. Similarly, the lowest dMn concentration was also  
 256 recorded in autumn. However, both the spring and summer experiments had similar initial dMn  
 257 concentrations. The calculated Mn\* values were high (0.16-0.25) with the lowest Mn\* observed in  
 258 autumn (Table 1).

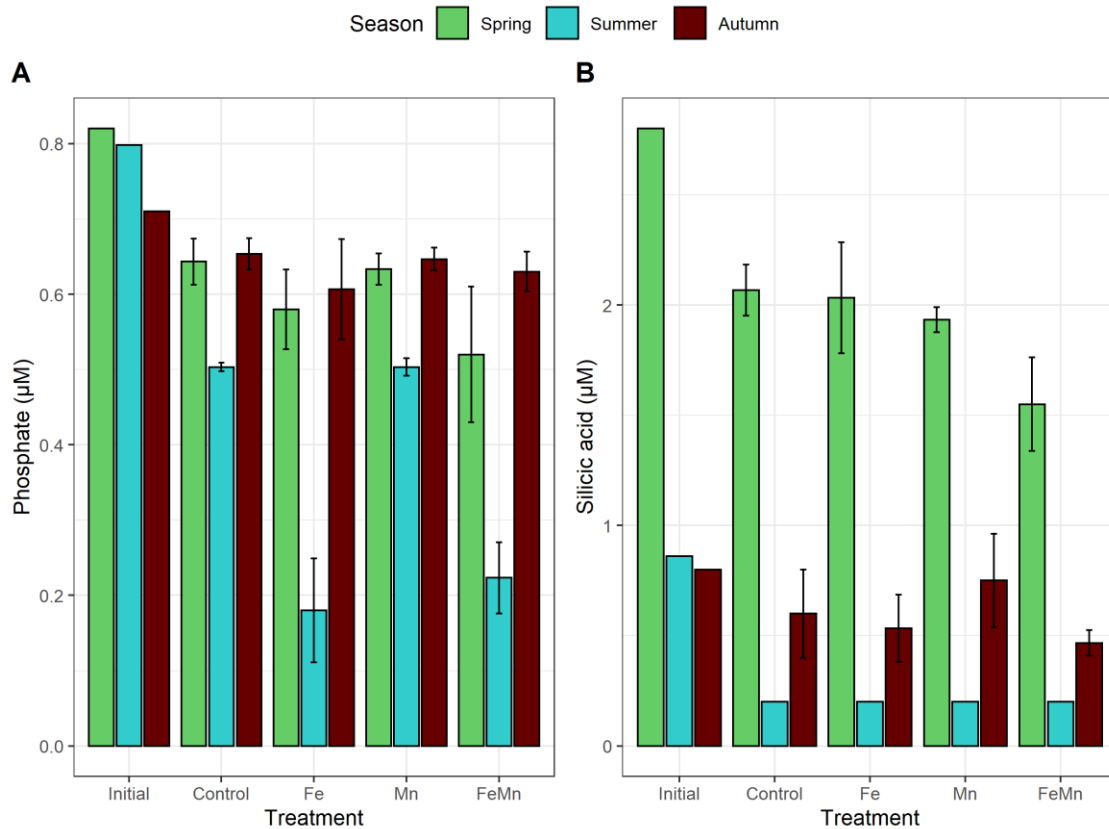
259 Table 1: Initial mean dFe and dMn concentrations with standard deviations measured in (or near) the seawater  
 260 incubated for the three experiments and the calculated Mn\* according to Browning et al. (2021): spring at PS2 in  
 261 2018 (n = 2), summer at SOTS in 2020 (n = 1) and autumn at SOTS in 2019 (n = 3). \*Single measurements were  
 262 performed for dFe and dMn in summer and dMn in autumn, in these cases the method error is indicated. In autumn,  
 263 both dFe and dMn values came from a near cast.

<b>Experiment</b>	<b>Spring (PS2)</b>	<b>Summer (SOTS)</b>	<b>Autumn (SOTS)</b>
<b>Depth of water collected (m)</b>	15	20	15
<b>dFe (nM)</b>	0.31 ± 0.001	0.50 ± 0.03*	0.15 ± 0.04
<b>dMn (nM)</b>	0.37 ± 0.032	0.44 ± 0.03*	0.26 ± 0.03*
<b>Mn*</b>	0.25	0.25	0.16

264

#### 265 MACRONUTRIENT DRAWDOWN

266 Both initial phosphate and silicic acid concentrations present in the seawater incubated for each  
 267 experiment, along with the final concentrations measured after 7 days of incubations are presented in  
 268 Figure 3. Focusing on the initial conditions, phosphate concentrations ranged from 0.71 to 0.82 μM,  
 269 with the lowest value observed in autumn and the highest in spring. Similarly, the lowest initial silicic  
 270 acid concentrations were observed in autumn (0.8 μM) and the highest in spring (2.8 μM).



271

272 Figure 3: Phosphate (A) and silicic acid (B) concentrations (µM) measured in the initial water incubated ("Initial"),  
 273 and after seven days of incubations for each treatment: Control ("Control"), +Fe ("Fe"), + Mn ("Mn"), +FeMn  
 274 ("FeMn"). The colour represents the season of the experiment: green for spring, blue for summer and brown for  
 275 autumn. Error bars represent the standard deviations and are smaller than the symbols when not visible (n = 3,  
 276 except for the initial treatment where n = 1).

277 Phosphate and silicic acid concentrations decreased over the 7-day incubation, across all seasons and  
 278 treatments. However, the uptake of both nutrients between each treatment varied seasonally. In spring,  
 279 no significant differences were observed by day 7 in phosphate and silicic acid concentrations, between  
 280 the control and the other treatments (ANOVA). In summer, we observed a significant decrease in  
 281 phosphate concentrations only in the treatments where Fe was added (+Fe and +FeMn), compared to  
 282 the control ( $p\text{-value} < 0.05$ , Tukey's HSD). No significant drawdown of phosphate was observed in the  
 283 Mn treatment, compared to the control. In summer, all treatments were characterized by final silicic  
 284 acid concentrations below the detection limit (0.2 µM). In autumn, no significant differences were  
 285 observed in either phosphate or silicic acid concentrations between treatments (ANOVA).

286 The uptake ratios for both phosphate and silicic acid differed seasonally (Table 2). In spring, no  
 287 significant differences in phosphate and silicic acid uptake rate were observed between treatments  
 288 (ANOVA). In summer, both Fe additions (+Fe and +FeMn) resulted in a very strong increase in the  
 289 phosphate uptake rate, which doubled compared to the control and Mn treatments ( $p\text{-value} < 0.05$ ,  
 290 Tukey's HSD). During this season, the treatment effects are impossible to interpret for the silicic acid  
 291 uptake rates as concentrations were drawn down below the detection limit (0.2 µM) (Figure 3 and Table

292 2). In autumn, we did not observe any significant differences in the uptake rates for either phosphate or  
 293 silicic acid between treatments (ANOVA).

294 Table 2: Average uptake rates of phosphate and silicic acid ( $\mu\text{M week}^{-1}$ ) and standard deviations for each treatment  
 295 calculated over the 7-day incubation period for each experiment (n=3). \*In summer, all final silicic acid  
 296 concentrations were below the detection limit (0.2  $\mu\text{M}$ ) and hence replaced with 0.2  $\mu\text{M}$ . Consequently, the  
 297 calculated uptake rate is identical in each treatment and cannot be interpreted.

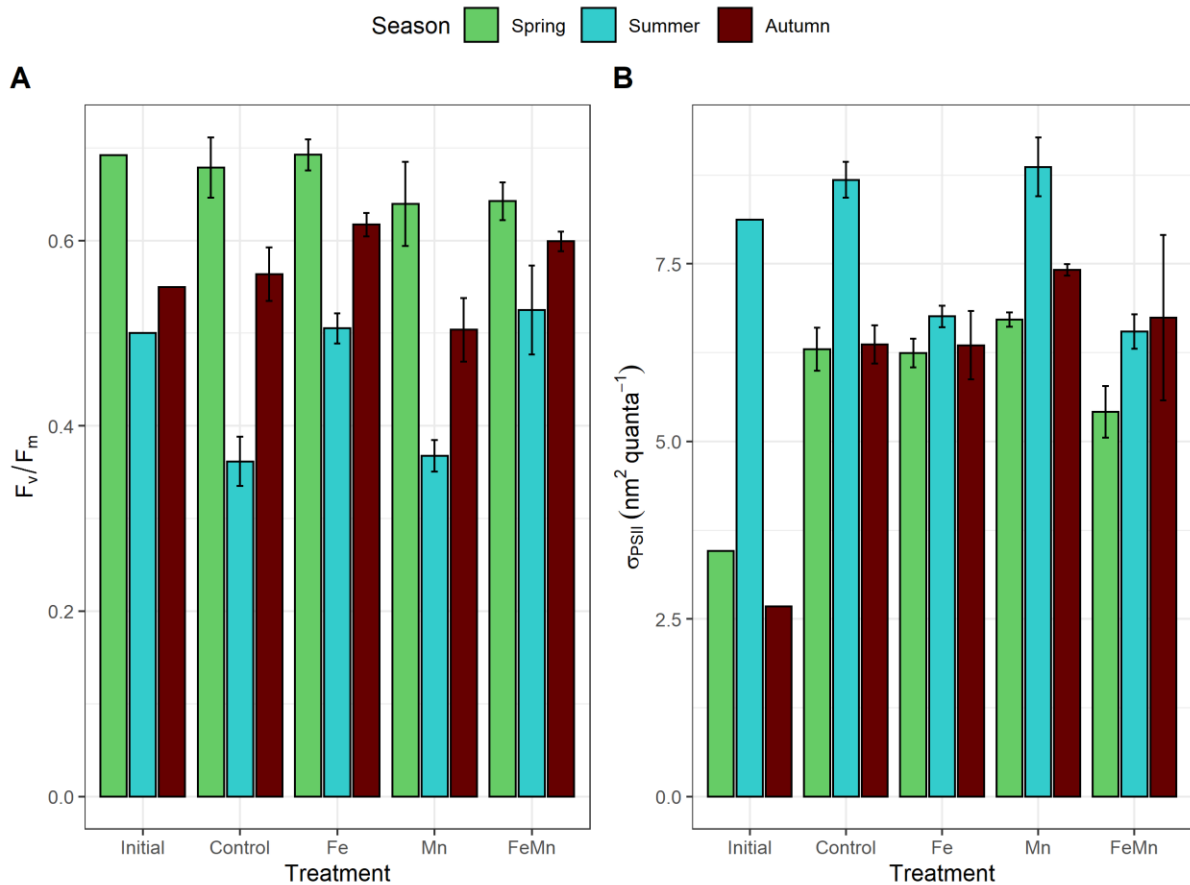
	Treatment	Control	+Fe	+Mn	+FeMn
<b>Phosphate</b>	Spring	0.18 $\pm$ 0.03	0.24 $\pm$ 0.05	0.19 $\pm$ 0.02	0.30 $\pm$ 0.09
	Summer	0.04 $\pm$ 0.001	0.09 $\pm$ 0.01	0.04 $\pm$ 0.002	0.08 $\pm$ 0.01
	Autumn	0.06 $\pm$ 0.02	0.10 $\pm$ 0.07	0.06 $\pm$ 0.02	0.08 $\pm$ 0.03
<b>Silicic acid</b>	Spring	0.73 $\pm$ 0.12	0.77 $\pm$ 0.26	0.87 $\pm$ 0.06	1.25 $\pm$ 0.21
	Summer	0.66* $\pm$ NA	0.66* $\pm$ NA	0.66* $\pm$ NA	0.66* $\pm$ NA
	Autumn	0.20 $\pm$ 0.20	0.27 $\pm$ 0.15	0.05 $\pm$ 0.20	0.33 $\pm$ 0.06

298

## 299 PHOTOPHYSIOLOGY

300 The photochemical efficiency of PSII ( $F_v/F_m$ ) differed between treatments and seasons (Figure 4A). In  
 301 spring, no significant differences in final  $F_v/F_m$  values were measured between treatments (ANOVA).  
 302 In summer, only the treatments with Fe additions (+Fe and +FeMn) maintained  $F_v/F_m$  values as high as  
 303 the initial community, and significantly higher than the control and +Mn treatments ( $p\text{-value} < 0.05$ ,  
 304 Tukey's HSD). In autumn, we measured significantly higher  $F_v/F_m$  values in both treatments with Fe  
 305 additions (+Fe and +FeMn) compared to the +Mn treatment ( $p\text{-value} < 0.05$ , Tukey's HSD). However,  
 306  $F_v/F_m$  values measured in both Fe treatments were not significantly higher than the control (ANOVA).

307 The functional absorption cross section of PSII ( $\sigma_{\text{PSII}}$ ) differed between seasons (Figure 4B). The initial  
 308 value was higher in summer compared to spring and autumn. In spring, we observed a significant  
 309 decrease in  $\sigma_{\text{PSII}}$  only in the +FeMn treatment, compared to the other treatments ( $p\text{-value} < 0.05$ ,  
 310 Tukey's HSD). In summer, both treatments with Fe additions (+Fe and +FeMn) were characterized by  
 311 a decrease in  $\sigma_{\text{PSII}}$  compared to the control and +Mn treatments ( $p\text{-value} < 0.05$ , Tukey's HSD). In  
 312 autumn, no significant differences in  $\sigma_{\text{PSII}}$  were observed between treatments (ANOVA).



313

314 Figure 4: A) Photochemical efficiency of photosystem II ( $F_v/F_m$ ) and B) functional absorption cross section of  
 315 PSII ( $\sigma_{PSII}$ ) in  $\text{nm}^2 \text{ quanta}^{-1}$ , measured for the initial algal communities incubated (“Initial”) and after 7 days of  
 316 incubation, in each treatment: Control, +Fe (“Fe”), + Mn (“Mn”), +FeMn (“FeMn”). The three colours show the  
 317 different seasons: green for spring, blue for summer and brown for autumn. Error bars represent the standard  
 318 deviations ( $n = 3$ , except for the initial treatment where  $n = 1$ ).

319 FLOW CYTOMETRY

320 Notable differences in phytoplankton community composition were observed between summer and  
 321 autumn. In summer, picoeukaryotes dominated the cell counts (Table 3). However, nanoeukaryotes  
 322 dominated community population size, as defined by equation (1) in the method section (Figure 5A).  
 323 In autumn, cyanobacteria dominated the counts (Table 3) while nanoeukaryotes dominated the  
 324 community population size (Figure 5B).

325 Table 3: Counts of phytoplankton cell ( $\text{cell mL}^{-1}$ ) measured in the main gated populations: picoeukaryotes  
 326 (“Picoeuk.”), cyanobacteria (“Cyano.”), nanoeukaryotes (“Nanos.”), large phytoplankton (“Large phyto.”) and  
 327 bacteria for the summer and autumn experiments, in each treatment. The mean value along with the standard  
 328 deviation ( $n=3$ ) is presented.

Summer					
Treatment	<i>Picoeuk.</i>	<i>Cyano.</i>	<i>Nanos.</i>	<i>Large phyto.</i>	<i>Bacteria</i>
Initial	10880	4150	5630	130	620400
Control	4820 ± 683	5517 ± 1142	15540 ± 560	213 ± 32	379703 ± 92672
Fe	4847 ± 3032	4980 ± 1802	21070 ± 2208	650 ± 191	401147 ± 32324

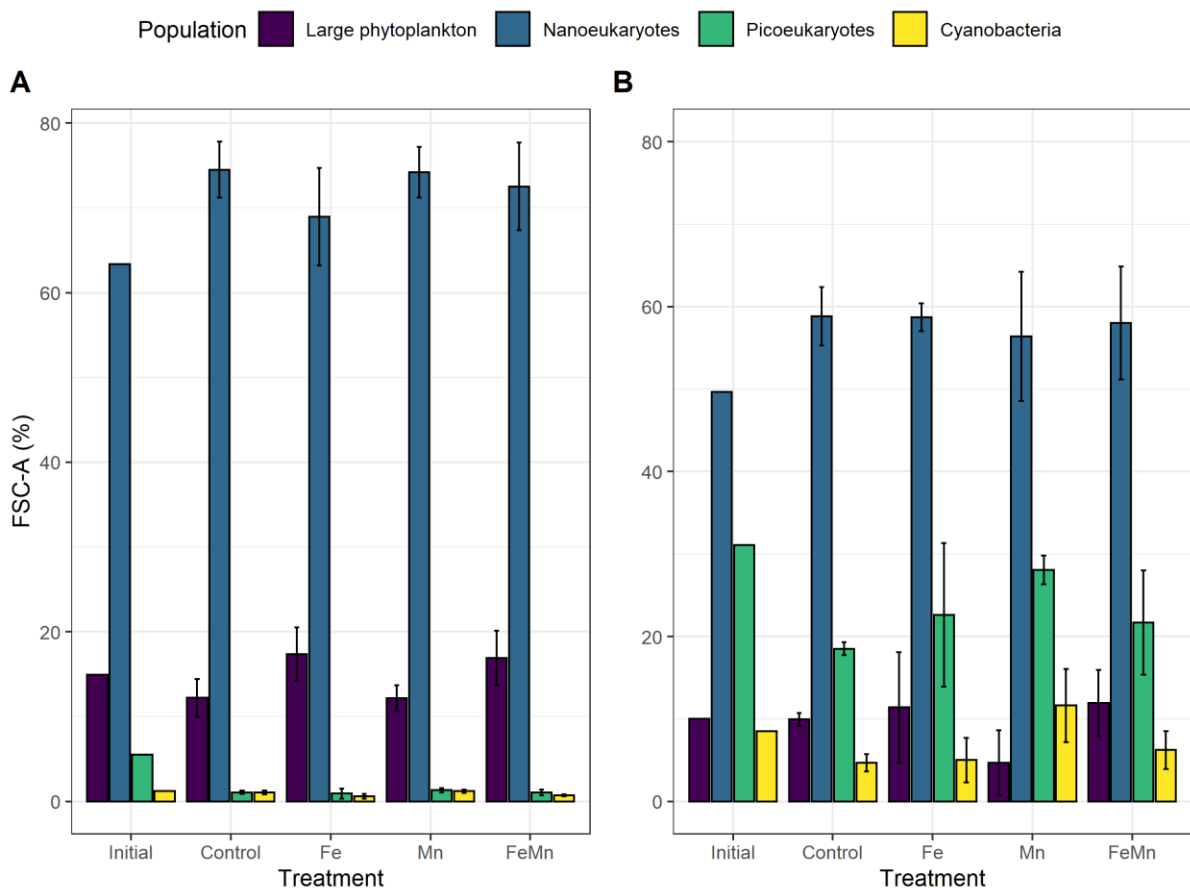
<b>Mn</b>	5203 ± 942	5883 ± 924	12430 ± 1311	170 ± 36	410350 ± 29142
<b>FeMn</b>	6317 ± 3163	5967 ± 1438	25593 ± 12130	593 ± 15	388403 ± 79888

**Autumn**

<b>Treatment</b>	<i>Pico.</i>	<i>Cyano.</i>	<i>Nano.</i>	<i>Large phyto.</i>	<i>Bacteria</i>
<b>Initial</b>	22230	25240	2260	80	655040
<b>Control</b>	12733 ± 3958	18743 ± 5479	4473 ± 2789	67 ± 21	734727 ± 123795
<b>Fe</b>	14220 ± 9869	27023 ± 2675	4230 ± 1897	77 ± 15	1080060 ± 764544
<b>Mn</b>	23865 ± 460	65405 ± 30823	4800 ± 891	55 ± 35	1280305 ± 323593
<b>FeMn</b>	12830 ± 1193	29450 ± 16046	4987 ± 876	117 ± 32	940517 ± 219637

329

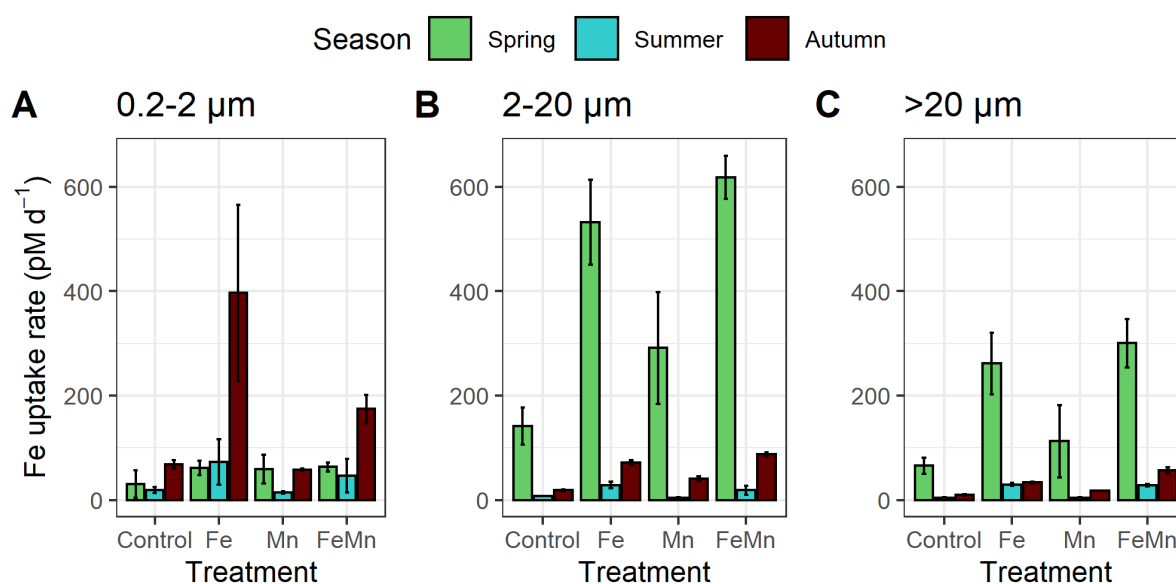
330 After 7 days of incubation, no significant difference in cell counts were observed between treatments  
 331 across seasons (ANOVA), but some small changes occurred in the sized-based metric. In autumn, the  
 332 addition of Mn led to an increase in the cyanobacteria population size relative to the whole  
 333 phytoplankton community ( $p$ -value < 0.05, Tukey's HSD). This change was not observed during the  
 334 summer experiment.



335 Figure 5: Relative contribution of four gated populations compared to all phytoplankton cells: large phytoplankton  
 336 (microeukaryotes), nanoeukaryotes, picoeukaryotes and cyanobacteria in terms of population size (FSC), as  
 337 defined in equation (1) for summer (A) and autumn (B). These values were calculated according to the equation  
 338 of Bach et al. (2018). Error bars represent the standard deviations (n = 3, except for the initial treatment where n  
 339 = 1).

340 IRON AND CARBON UPTAKE

341 Different rates of Fe uptake were observed between seasons and size fractions (Figure 6). Focusing on  
 342 the 0.2-2  $\mu\text{m}$  size fraction, no significant differences were observed between treatments across seasons.  
 343 However, in summer and autumn, Fe uptake rates increased under Fe additions, with higher average  
 344 values in the +Fe addition alone. The highest Fe uptake was observed in autumn ( $396.8 \pm 169 \text{ pM d}^{-1}$ ),  
 345 whereas mean Fe uptake was lower when both Fe and Mn were added ( $174.6 \pm 27 \text{ pM d}^{-1}$ ). No  
 346 significant difference was observed between treatments in autumn, likely resulting from a small  
 347 dataset (only 2 datapoints for the +Fe treatment).



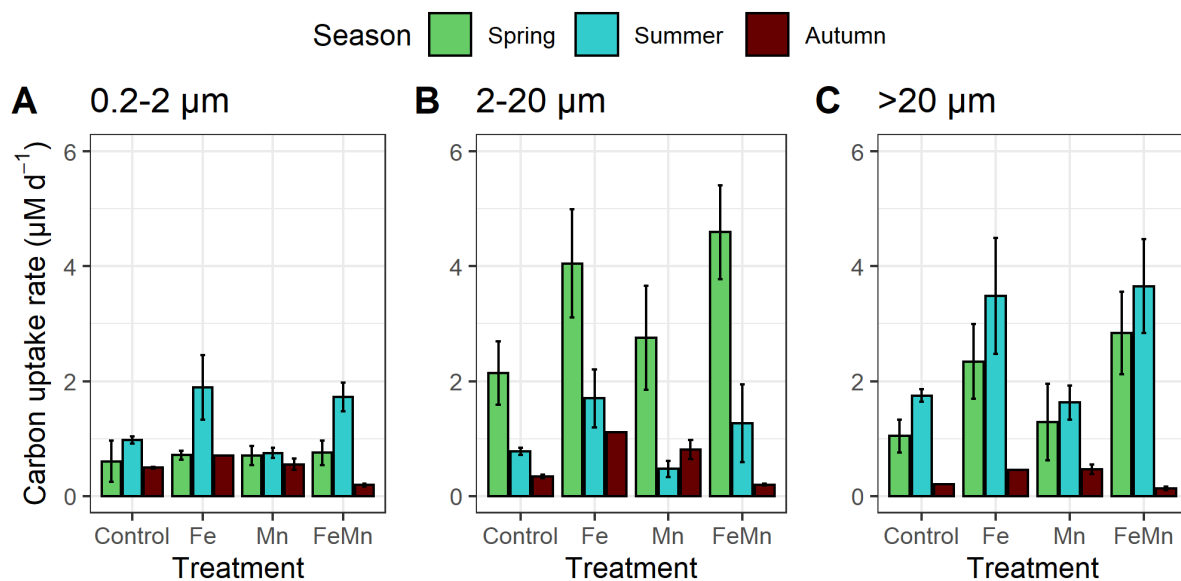
348  
 349 Figure 6: Fe uptake ( $\text{pM d}^{-1}$ ) measured in each size fraction and for the three seasons: spring in green, summer in  
 350 blue and autumn in brown. During the autumn experiment, only two datapoints were recorded for the +Fe  
 351 treatment. Error bars represent the standard deviations and are smaller than the symbols when not visible ( $n = 3$ ).

352 In the 2-20  $\mu\text{m}$  size class (Figure 6B), Fe uptake was highest in spring with significantly higher Fe  
 353 uptake under both Fe additions compared to the control and +Mn treatments ( $p\text{-value} < 0.05$ , Tukey's  
 354 HSD). The +Mn treatment induced an increase in Fe uptake. However, it was not significantly higher  
 355 than the control. In comparison, both summer and autumn seasons were characterized by much lower  
 356 Fe uptake in the 2-20  $\mu\text{m}$  size fraction. In summer, Fe uptake rates were significantly higher than the  
 357 control only in the +Fe treatment, with a mean value four times higher than Fe uptake in the control ( $p\text{-value} < 0.05$ , Tukey's HSD). The combined +FeMn addition did not result in a significant stimulation  
 358 of Fe uptake compared to the control ( $p\text{-value} = 0.06$ , Tukey's HSD). In autumn, no significant  
 359 differences in Fe uptake were observed between treatments (Kruskal-Wallis test).

361 The >20  $\mu\text{m}$  size class (Figure 6C) was also characterized by higher Fe uptake values measured in the  
 362 spring. In both spring and summer, Fe uptake was significantly higher in both treatments with Fe  
 363 additions (+Fe and +FeMn), compared to the control and +Mn treatments ( $p\text{-value} < 0.05$ , Tukey's

364 HSD). In autumn, no significant differences in Fe uptake were observed between treatments, which  
 365 could result from a low number of data points (Kruskal-Wallis test).

366 Net primary productivity, measured through carbon uptake, also strongly varied between seasons and  
 367 size fractions (Figure 7). In spring, no significant difference in carbon uptake rates were observed  
 368 between treatments in the small size fraction (ANOVA). In summer, we measured the highest carbon  
 369 uptake for picoeukaryotes in the +Fe treatment compared to the control ( $p$ -value < 0.05, Tukey's HSD).  
 370 In addition, both Fe treatments (+Fe and +FeMn) had significantly higher carbon uptake rates than the  
 371 +Mn treatment ( $p$ -value < 0.05, Tukey's HSD). In autumn, no significant differences in carbon uptake  
 372 were observed in the 0.2-2  $\mu$ m size class (Kruskal-Wallis test).



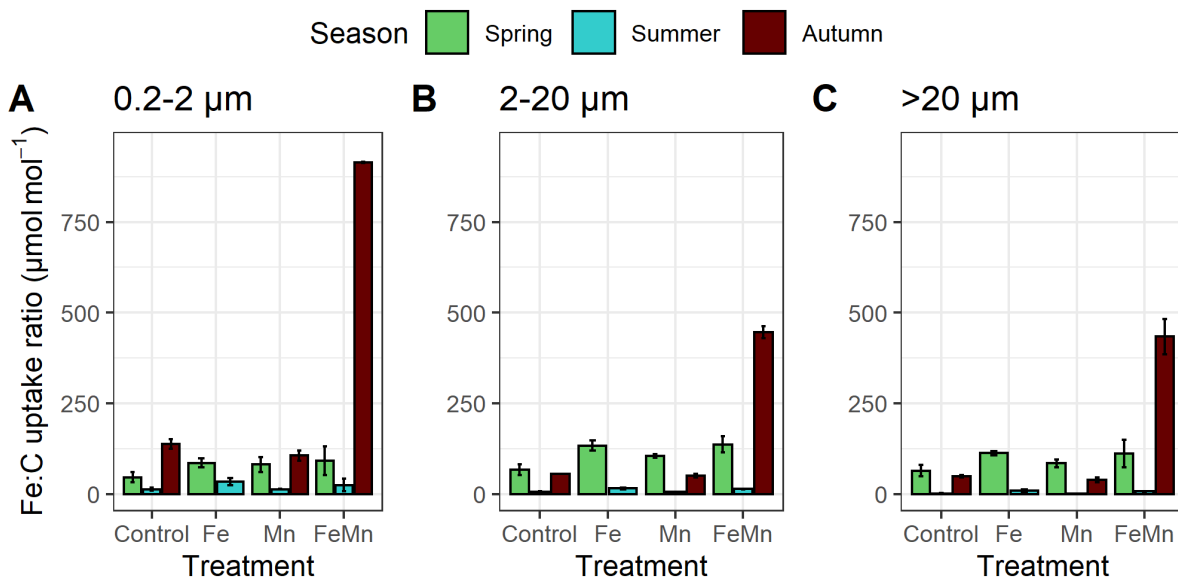
373  
 374 Figure 7: Carbon uptake ( $\mu\text{M d}^{-1}$ ) measured in each size fraction and for the three seasons: spring in green, summer  
 375 in blue and autumn in brown. Due to a manipulation mistake during the autumn experiment, only one datapoint  
 376 was recorded for the +Fe treatment. For the other treatments, error bars represent the standard deviations and are  
 377 smaller than the symbols when not visible ( $n = 3$ ).

378 For the nanoeukaryotes (2-20  $\mu\text{m}$ ) during the spring season, only the +FeMn treatment had higher  
 379 carbon uptake rates than the control ( $p$ -value < 0.05, Tukey's HSD). In summer, a significant difference  
 380 between carbon uptake was only observed between the +Fe and +Mn treatments ( $p$ -value < 0.05,  
 381 Tukey's HSD), with higher carbon uptake with Fe addition alone. In autumn, no significant differences  
 382 were observed between treatments (Kruskal-Wallis test).

383 In the >20  $\mu\text{m}$  size class, there was no significant difference in carbon uptake between treatments in  
 384 spring (Kruskal-Wallis test). In summer, carbon uptake was only significantly higher in the +FeMn  
 385 treatment compared to the control treatment ( $p$ -value < 0.05, Tukey's HSD). The carbon uptake rates  
 386 measured in the +Fe treatment, while elevated, were not significantly different than the control ( $p$ -value  
 387 = 0.05, Tukey's HSD). However, both +Fe and +FeMn treatments had a higher carbon uptake than in

388 the +Mn treatment ( $p$ -value  $< 0.05$ , Tukey's HSD). In autumn, no significant differences were observed  
389 in the carbon uptake between treatments within this size class (Kruskal-Wallis test).

390 Iron to carbon (Fe:C) uptake ratios differed between seasons and treatments, with overall higher ratios  
391 measured in autumn (Figure 8). Across all sizes, Fe:C ratio ranged between 33 to 153  $\mu\text{mol mol}^{-1}$  in  
392 spring, 1 to 18  $\mu\text{mol mol}^{-1}$  in summer and from 34 to 915  $\mu\text{mol mol}^{-1}$  in autumn. In the 0.2-2  $\mu\text{m}$  size  
393 fraction, no significant differences were observed between treatments across seasons (ANOVA for  
394 spring and summer; and Kruskal-Wallis test for autumn).



395

396 Figure 8: Iron to carbon (Fe:C) uptake ratio ( $\mu\text{mol mol}^{-1}$ ) measured in each size fraction and for the three seasons:  
397 spring in green, summer in blue and autumn in brown. The Fe:C ratio from the +Fe treatment in autumn was not  
398 included due to missing data. Error bars represent the standard deviations and are smaller than the symbols when  
399 not visible ( $n = 3$ ).

400 For the nanoeukaryotes (2-20  $\mu\text{m}$ ), spring Fe:C uptake ratios were higher in +Fe and +FeMn treatments  
401 compared to the control treatment ( $p$ -value  $< 0.05$ , Tukey's HSD). In summer, Fe:C ratios measured in  
402 +Fe and +FeMn treatments were higher than ratios measured in both the control and +Mn treatments  
403 ( $p$ -value  $< 0.05$ , Tukey's HSD). In autumn, no significant differences were observed, likely resulting  
404 from a small dataset (Kruskal-Wallis test).

405 No significant differences in Fe:C uptake ratios for the microeukaryotes (>20  $\mu\text{m}$ ) were observed during  
406 the spring experiment (ANOVA), while Fe:C ratios were higher under +Fe and +FeMn compared to  
407 the control and +Mn treatments in summer ( $p$ -value  $< 0.05$ , Tukey's HSD). In autumn, no significant  
408 differences were observed but again, this may result from a small dataset (Kruskal-Wallis test).

## 409 Discussion

### 410 CONTRASTING HYDROGRAPHIC SITES

411 Contrasting results may be expected between experiments due to the different locations of the spring  
412 experiment, done at PS2, and the two other experiments (summer and autumn), performed at SOTS.  
413 The intrusion of warmer and saltier waters from the subtropical zone are commonly observed in the  
414 northern part of the subantarctic zone near SOTS and can originate from either the mixing with waters  
415 from the Zeehan Current or mixing with waters and eddies from the East Australian Current (Bowie et  
416 al. 2011). In this study, the PS2 station, located southeast of Tasmania, is much more likely to be  
417 influenced by the East Australian Current, compared to the SOTS site. This explains the strong  
418 difference in salinity observed in the spring experiment compared to the two other experiments.  
419 However, autonomous seasonal records of phytoplankton communities from the SOTS station revealed  
420 no change in community composition due to the input of subtropical waters in the subantarctic zone  
421 (Eriksen et al. 2018). Hence, we suggest that the results of the three experiments are comparable, despite  
422 the influence of subtropical waters at PS2 in the spring experiment.

423 The three experiments undertaken were characterized by different initial macronutrient concentrations.  
424 Higher phosphate and silicic acid concentrations were observed at the beginning of the spring  
425 experiment, which is a characteristic of the early season following winter mixing of surface waters  
426 (Rintoul and Trull 2001). In contrast, macronutrient concentrations were lowest in autumn. Phosphate  
427 concentrations decrease during the summer season due to biological uptake but are expected to remain  
428 higher than limiting levels (Rintoul and Trull 2001). On the other hand, silicic acid concentrations  
429 decrease during the growth season, due to consumption from silicifying phytoplankton such as diatoms,  
430 silicoflagellates and radiolarians (Deppeler and Davidson 2017; Eriksen et al. 2018). In autumn, silicic  
431 acid concentrations reached limiting levels, down to 0.8  $\mu\text{M}$  (Paasche 1973; Hutchins et al. 2001;  
432 Westwood et al. 2011). Therefore, silicic acid growth limitation of silicifying organisms may be  
433 expected during the autumn experiment. Nitrate concentrations are not presented here but initial levels  
434 were not considered limiting (nitrate + nitrite: 11.0  $\mu\text{M}$  in spring, 10.2  $\mu\text{M}$  in summer, 8.3  $\mu\text{M}$  in  
435 autumn).

436 Initial trace metal concentrations were highest in spring for dMn and summer for dFe. It is surprising  
437 to observe higher summer dFe concentrations compared to the spring experiment. Usually, higher  
438 dissolved concentrations are recorded in the early season, resulting from i) aerosol depositions coming  
439 from proximal land (Perron et al. 2020), ii) southern advection of Fe and Mn enriched subtropical waters  
440 from the East Australian Current (Sedwick, et al. 2008; Bowie et al. 2009) and/or iii) replete trace metal  
441 levels present after the winter season associated with wind-mixing (Bowie et al. 2009). At the SOTS  
442 site, higher dFe concentrations observed in summer may result from entrainment following wind-

443 mixing events while decreasing autumn concentrations for both elements likely result from biological  
444 consumption.

445 Initial phytoplankton biomass in summer and autumn was dominated by pico- and nanoplankton, as  
446 previously observed in this subantarctic region (Fourquez et al. 2020). In summer, picoeukaryotes  
447 dominated phytoplankton abundance while picocyanobacteria were relatively important in autumn  
448 (Figure 5). It is likely that *Synechococcus* sp. dominated the picocyanobacteria, as has been previously  
449 observed at SOTS (Cassar et al. 2015; Fourquez et al. 2020). In all seasons, *in-situ* light limitation of  
450 phytoplankton growth is expected due to the deep mixed layer depths present (Figure 2). Indeed, Rintoul  
451 and Trull (2001) previously observed that a mixed layer depth of 75 to 100 m was deep enough to light  
452 limit phytoplankton growth in this region. Here, the mixed layer depth was at or  $\geq 100$  m (Figure 2).  
453 Initial physiological measurements indicated that the bulk phytoplankton communities were relatively  
454 healthy ( $F_v/F_m > 0.5$ ) at all seasons (Figure 4). However, our data indicated various degrees of Fe  
455 limitation.

#### 456 SEASONALITY OF IRON LIMITATION

457 Phytoplankton growth in subantarctic waters is usually assumed to be Fe limited (Boyd et al. 1999;  
458 Sedwick et al. 1999; Hutchins et al. 2001; Petrou et al. 2011). However, our experiments demonstrate  
459 that the degree of Fe limitation is seasonal. A previous review suggested Fe may limit subantarctic  
460 phytoplankton communities in spring (Boyd 2002). Contrasting with this hypothesis, no clear evidence  
461 of Fe stress was observed in our spring experiment. This may result from relatively elevated dFe  
462 concentrations in the early season, sufficient to maintain optimal phytoplankton growth at that time.  
463 This was supported by the high  $F_v/F_m$  values measured in all treatments (Figure 4A), suggesting efficient  
464 light utilization in PSII (Greene et al. 1992; Hopkinson and Barbeau 2008). Unfortunately, the lack of  
465 flow cytometry data for this season means that the initial composition of the phytoplankton community  
466 and how it evolved with Fe and Mn additions were not assessed. Previous reports showed this  
467 subantarctic region is characterized by a succession from large diatoms in spring toward weakly  
468 silicified diatoms in summer/autumn (Eriksen et al. 2018). From our Fe and carbon uptake results, it  
469 was observed that most of the Fe and carbon uptake came from nano- and microplankton in spring  
470 (Figure 6 and 7). Hence, it is possible the spring experiment took place during the transition from large  
471 diatoms ( $> 20 \mu\text{m}$ ) toward smaller (2-20  $\mu\text{m}$ ) and more weakly silicified diatoms in response to  
472 decreasing ambient dFe and silicic acid concentrations (Eriksen et al. 2018).

473 The strongest signal of Fe limitation was observed during the summer experiment as highlighted by i)  
474 the drawdown of phosphate concentrations in both treatments where Fe was added (Figure 3A), and ii)  
475 the increase  $F_v/F_m$  and the decrease in  $\sigma_{\text{PSII}}$  with Fe additions (Figure 4). These results suggest that the  
476 addition of Fe alleviated phytoplankton stress (Greene et al. 1992; Petrou et al. 2011) and agreed with  
477 previous suggestion of dominant Fe limitation in summer (Boyd 2002). Although nitrate levels were

478 greatly drawn down by the end of the experiment within both Fe treatments (between 0.6 to 2  $\mu\text{M}$  in 5  
479 replicate bottles, and down to < detection limit levels in 1 replicate bottle), co-limitation from Fe and  
480 silicic acid may more likely occur toward the end of the experiment due to ongoing nutrient  
481 consumption (Figure 3B). Flow cytometry results indicated that nanoeukaryotes dominated the initial  
482 population size and remained the dominant group throughout the experiment in all treatments (Figure  
483 5A). Combined with the high uptake of silicic acid observed in summer (Figure 3B), these results  
484 suggest the growth stimulation of relatively small diatoms, within the nanoeukaryote size range, in  
485 agreement with previous results (Eriksen et al. 2018). Despite an overall dominance of smaller diatoms,  
486 large phytoplankton (>20  $\mu\text{m}$ ) dominated primary productivity (Figure 7C). Microeukaryotes  
487 comprised about 15% of the population size (Figure 5) and may be composed of large diatoms and large  
488 dinoflagellates, as previously observed in subantarctic waters (Cassar et al. 2015; Eriksen et al. 2018).  
489 Coincident with this relatively high carbon uptake, very low Fe uptake rates were measured in both the  
490 nano- and micro- size classes, which suggest that these large summer phytoplankton species, likely  
491 diatoms, have low cellular Fe requirements (Strzepek et al. 2011; Gao et al. 2021). This assertion was  
492 supported by the very low Fe:C uptake ratios observed during summer in all size classes (Figure 8),  
493 implying that diatoms were able to sustain growth and substantial carbon assimilation with very low Fe  
494 requirements. Similarly, it is notable that the 0.2-2  $\mu\text{m}$  size class had carbon uptake rates as high as the  
495 2-20  $\mu\text{m}$  size fraction, implying a similar efficiency in assimilating carbon between both size classes  
496 (Figure 7). However, relatively higher Fe uptake rates observed in the 0.2-2  $\mu\text{m}$  size class may indicate  
497 higher efficiency in Fe uptake, possibly due to their lower surface area volume ratio (Sunda and  
498 Huntsman 1995; Strzepek et al. 2011). Notably, this size fraction also includes Fe uptake by  
499 heterotrophic bacteria but their contribution to Fe uptake was not determined.

500 In autumn, Fe limitation was evident, supported by the increase in  $F_v/F_m$  with Fe addition (Figure 4;  
501 +Fe treatment only) but to a lesser extent than in summer. In contrast to the summer experiment,  
502 phosphate and silicic acid drawdown remained much lower in autumn (Table 2), indicating that a factor  
503 other than Fe may be (co-)limiting phytoplankton growth. Given the low initial silicic acid levels  
504 observed (0.8  $\mu\text{M}$ ), silicic acid may be the primary variable limiting the growth of silicified organisms  
505 (Hutchins et al. 2001; Eriksen et al. 2018) and not dFe concentrations or other macronutrients  
506 considering phosphate (0.71  $\mu\text{M}$ ) and nitrate + nitrite levels (8.3  $\mu\text{M}$ ) remained above limiting levels  
507 (Sedwick et al. 1999; Rintoul and Trull 2001). However, the possibility of Fe and silicic acid co-  
508 limitation of diatoms growth cannot be excluded (Boyd 2002). A previous study in the subantarctic  
509 zone suggested a seasonal succession of limiting variables, with both Fe and silicic acid concentrations  
510 limiting the growth of heavily silicified diatoms in late summer and autumn, leading to a community  
511 shift toward non-silicified and/or lightly silicified diatoms with low Fe requirements (Hutchins et al.  
512 2001). Relatively high Fe uptake rates were measured in all size classes during the autumn experiment  
513 compared to summer (Figure 6), possibly due to an upregulation of Fe acquisition in response to chronic

514 Fe limitation in these late season phytoplankton communities. In the >20  $\mu\text{m}$  size class, it is possible  
515 dinoflagellates dominated phytoplankton abundance as silicic acid levels were likely limiting the  
516 growth of large diatoms (Eriksen et al. 2018). Unfortunately, we cannot confirm the phytoplankton  
517 community composition of the medium and small size class as additional information would be  
518 necessary, such as pigments analyses or microscopy. Flow cytometry did allow the identification of  
519 picocyanobacteria, which represented an important group during this season.

520 In autumn, picocyanobacteria, most likely *Synechococcus* sp. (Cassar et al. 2015) numerically  
521 dominated the phytoplankton community (Table 3). Previous flow cytometric analyses showed  
522 picocyanobacteria are a significant group within the subantarctic phytoplankton community,  
523 contributing about 20% to total phytoplankton biomass in mid-late summer (Cassar et al. 2015). In  
524 autumn, the contribution of picocyanobacteria to the population size doubled with +Mn addition (Figure  
525 5). The photophysiology of picocyanobacteria differs from diatoms and other major phytoplankton  
526 groups (Suggett et al. 2009). This is mostly due to their use of phycobilisomes as light-harvesting  
527 pigments which results in lower maximum PSII photochemical efficiency (Suggett et al. 2004).  
528 Previous studies reported  $F_v/F_m$  values ranging from 0.1 to 0.6 for picocyanobacteria (Campbell et al.  
529 1998; Koblížek et al. 2001; Suggett et al. 2009). Hence, it is not straight-forward to link relatively low  
530  $F_v/F_m$  values with Fe limitation within a phytoplankton community dominated by cyanobacteria. The  
531 increase in  $F_v/F_m$  observed in the +Fe treatment (Figure 4A) may indicate that a different population  
532 with an intrinsically higher  $F_v/F_m$  responded to Fe addition. The slightly higher silicic acid uptake rates  
533 observed with Fe additions (Table 2) suggest the growth of silicified organisms, possibly weakly  
534 silicified diatoms in this late season. However, it was previously shown that picocyanobacteria can  
535 accumulate silicon intracellularly as a hydrated siliceous network, associated with magnesium or  
536 calcium (Ohnemus et al. 2018). Hence, the higher silicic acid uptake may have also resulted from  
537 picocyanobacteria stimulation. These results highlight the complexity of identifying nutrient stress  
538 conditions from a bulk phytoplankton community dataset, where signals from specific taxonomic  
539 groups can get easily lost (Suggett et al. 2009). However, our findings provide evidence for a strong  
540 seasonality of Fe limitation and a seasonal succession of various phytoplankton groups, associated with  
541 their responses to key environmental constraints, particularly dFe and silicic acid concentrations  
542 (Eriksen et al. 2018). In addition, seasonality in phytoplankton responses to Mn additions were also  
543 observed.

#### 544 EVIDENCE OF IRON-MANGANESE CO-LIMITATION

545 Overall, these seasonal experiments did not show a clear signal of Fe-Mn co-limitation, in comparison  
546 to the strong responses observed from Fe additions. This outcome concurred with the high  $\text{Mn}^*$  values  
547 calculated for the three seasons (Table 1), fitting within the range of Browning et al. (2021) (0.16 -0.31  
548 nM) for which Fe was limiting but not Mn. However, we observed some interesting responses to Mn  
549 addition, particularly from picocyanobacteria. In autumn, the addition of Mn noticeably stimulated the

550 growth of picocyanobacteria (Figure 5). The lower bulk  $F_v/F_m$  value observed in this treatment may  
551 support the hypothesis of a dominant contribution from cyanobacteria, which often have an intrinsically  
552 lower  $F_v/F_m$  than eukaryotic algae (Campbell et al. 1998; Koblížek et al. 2001; Suggett et al. 2009). The  
553 stimulation of the picocyanobacterial population under Mn addition may indicate that Mn was limiting  
554 cyanobacterial growth. However, the  $F_v/F_m$  parameter is not a reliable indicator of PSII efficiency in  
555 cyanobacteria as they have more flexible electron transport systems (Campbell et al. 1998) and PSII is  
556 poorly excited by the wavelength (470 nm) used in this study. Cyanobacterial Mn requirements are still  
557 poorly understood. Previous laboratory studies of *Synechocystis* (a freshwater cyanobacteria) showed  
558 that dMn concentrations  $\leq 100$  nM reduces oxygen evolution capacity and results in the accumulation  
559 of partially assembled PSII systems, and changes in the organization of photosystem I complexes  
560 (Salomon and Keren 2011). In their most limiting Mn treatment, Salomon and Keren (2011) measured  
561 a background dMn concentration of 1.8 nM, which is still much higher than what is commonly observed  
562 in Southern Ocean open waters. However, oceanic strains may have adapted to lower surrounding dMn  
563 concentrations by lowering their Mn requirements. This was previously shown in cyanobacteria  
564 regarding adaptation to Fe limitation (Ferreira and Straus 1994). Twining et al. (2010) reported Mn cell  
565 quotas (normalised to phosphate) ranging from 0.46 to 0.81 mmol/mol in *Synechococcus* sp. cells from  
566 the Sargasso Sea, with strong variations between cyclonic/anticyclonic eddies and mode waters. In Fe-  
567 limited Southern Ocean waters, for which there are no data on cyanobacteria, much lower Mn to  
568 phosphate ratios were measured in autotrophic flagellates and, unlike diatoms, the ratio increased once  
569 Fe stress was alleviated (Twining et al. 2004). Overall, there is insufficient information on the Mn  
570 requirements of subantarctic cyanobacterial strains to predict the dMn concentrations at which they  
571 become limited. However, our results provide the first evidence that Mn may limit cyanobacteria growth  
572 in autumn, when small picoplankton dominate the biomass and surrounding dMn concentrations are  
573 lowest. This implies Mn may be linked to deep carbon export as cyanobacteria have been observed to  
574 significantly contribute to downward carbon export in subantarctic waters through aggregation (Waite  
575 et al. 2000; Cassar et al. 2015) which increases their sinking rate (Jackson 2005). Hence, there may be  
576 seasonality in the importance of Mn in stimulating phytoplankton growth, associated with specific  
577 phytoplankton taxa such as cyanobacteria.

578 Another interesting result associated with Mn additions was the significant stimulation of carbon uptake  
579 within the 2-20  $\mu\text{m}$  size class in spring and within the  $>20$   $\mu\text{m}$  size class in summer, only occurring  
580 under combined Fe and Mn additions (Figure 7). Increased carbon fixation and hence, photosynthesis,  
581 suggest that these size classes of the phytoplankton community benefited from the combined addition  
582 and may be Fe-Mn co-limited. Phytoplankton Mn requirements are directly linked to photosynthesis by  
583 two processes: i) the number of PSII reaction centres, due to the central role of Mn in the oxygen-  
584 evolving complex of PSII (Armstrong 2008) and, ii) the need for Mn to produce the superoxide  
585 dismutase enzyme, to detoxify the cell of superoxide produced during photosynthesis (Peers and Price

586 2004; Wolfe-Simon et al. 2006). Increased Mn requirements were previously observed in Fe-limited  
587 diatoms, due to additional ROS production associated with Fe limitation (Peers and Price 2004). Hence,  
588 stimulation of carbon uptake observed under combined Fe and Mn additions during the summer  
589 experiment may be linked to ROS production and increased Mn requirement, knowing that  
590 phytoplankton communities were strongly Fe-limited (see previous section). Conversely, stimulation  
591 of carbon fixation measured under combined addition in spring is surprising considering phytoplankton  
592 communities were not Fe-limited. Instead, this enhanced carbon fixation may result from higher Mn  
593 demands associated with higher Fe requirements observed in these early phytoplankton communities.

594 Our results support the hypothesis that Mn concentrations may be low enough to limit the growth of a  
595 subset of the primary producers in this subantarctic region and hence to influence phytoplankton  
596 community composition. However, these effects appear to vary seasonally, and are subtle. Here, the  
597 evaluation of primary productivity through size-fractionated carbon uptake measurements coupled with  
598 flow cytometry helped us to identify these co-limitation signals but this approach is not commonly used.  
599 This highlights the need to use a combination of existing techniques, and to develop new tools, to  
600 identify Mn (co-)limitation within subpopulations of the phytoplankton community.

## 601 Conclusion

602 In conclusion, the signal of Mn (co-)limitation observed during these multi-seasonal experiments was  
603 masked by the strong seasonality and responses associated with Fe limitation. Our results suggest spring  
604 Fe and Mn concentrations were high enough to not limit phytoplankton growth. Conversely,  
605 phytoplankton communities were strongly Fe limited in summer. In autumn, we suggest low silicic acid  
606 levels limited diatom growth. However, the possibility that silicic acid and Fe were co-limiting diatom  
607 growth cannot be excluded. Manganese additions induced subtle community and physiological changes.  
608 In autumn, the addition of Mn alone stimulated the growth of cyanobacteria, most likely *Synechococcus*  
609 sp. These results suggest cyanobacteria may be Mn-limited in autumn when they constitute an important  
610 part of resident phytoplankton biomass and dMn concentrations are lowest following the phytoplankton  
611 growth season. In spring and summer, combined Fe and Mn additions stimulated carbon fixation in the  
612 nano- and micro- size classes, respectively. This was hypothesized to be due to the high Mn  
613 requirements of the spring community and ROS production linked to Fe limitation in summer. These  
614 results indicate that Mn may play an important role in controlling/stimulating specific phytoplankton  
615 taxa, with seasonal variability. In addition, our results show that Mn (co-)limitation signal may be hard  
616 to capture in conventional bioassays, especially when pronounced Fe responses are observed.

## 617 Acknowledgements

618 We would like to acknowledge the officers and crew of the RV *Investigator* (Australian Marine National  
619 Facility) for the deployment of all the instruments during the three voyages (IN2018-V04; IN2019-V02  
620 and IN2020-V08), and the hydro-chemistry team who performed the macronutrients analyses onboard.

621 We thank Pamela Barrett and Robin Grun for the collection and analyses of trace metal samples  
622 performed for the first two voyages. This work was funded through the Antarctic Climate & Ecosystems  
623 Cooperative Centre (ACE CRC) and by the Australian Antarctic Program Partnership (AAPP).

## 624 References

- 625 Armstrong, F. A. 2008. "Why Did Nature Choose Manganese to Make Oxygen?" *Philosophical*  
626 *Transactions of the Royal Society B: Biological Sciences* 363 (1494): 1263–70.  
627 <https://doi.org/10.1098/rstb.2007.2223>.
- 628 Bach, L. T., Lohbeck, K. T., Reusch, T. B., and U. Riebesell. 2018. "Rapid Evolution of Highly  
629 Variable Competitive Abilities in a Key Phytoplankton Species." *Nature Ecology &*  
630 *Evolution* 2 (4): 611–13. <https://doi.org/10.1038/s41559-018-0474-x>.
- 631 Bowie, A. R., F. Griffiths, B., Dehairs, F., and T. W. Trull. 2011. "Oceanography of the Subantarctic  
632 and Polar Frontal Zones South of Australia during Summer: Setting for the SAZ-Sense  
633 Study." *Deep Sea Research Part II: Topical Studies in Oceanography* 58 (21–22): 2059–70.  
634 <https://doi.org/10.1016/j.dsr2.2011.05.033>.
- 635 Bowie, A. R., Lannuzel, D., Remenyi, T. A., Wagener, T., Lam, P. J., Boyd, P. W., Guieu, C.,  
636 Townsend, A. T., and T. W. Trull. 2009. "Biogeochemical Iron Budgets of the Southern  
637 Ocean South of Australia: Decoupling of Iron and Nutrient Cycles in the Subantarctic Zone  
638 by the summertime supply." *Global Biogeochemical Cycles* 23 (4): n/a-n/a.  
639 <https://doi.org/10.1029/2009GB003500>.
- 640 Boyd, P. W., LaRoche, J., Gall, M., Frew, R., and R. M. L. McKay. 1999. "Role of Iron, Light, and  
641 Silicate in Controlling Algal Biomass in Subantarctic Waters SE of New Zealand." *Journal of*  
642 *Geophysical Research: Oceans* 104 (C6): 13395–408. <https://doi.org/10.1029/1999JC900009>.
- 643 Boyd, P. W. 2002. "Environmental factors controlling phytoplankton processes in the Southern  
644 Ocean." *Journal of Phycology* 38 (5): 844–861.
- 645 Boyd, P. W., Watson, A. J., Law, C. S., Abraham, E. R., Trull, T., Murdoch, R., Bakker, D. C. E., et  
646 al. 2000. "A Mesoscale Phytoplankton Bloom in the Polar Southern Ocean Stimulated by Iron  
647 Fertilization." *Nature* 407 (6805): 695–702. <https://doi.org/10.1038/35037500>.
- 648 Browning, T. J., Achterberg, E. P., Engel, A., and E. Mawji. 2021. "Manganese Co-Limitation of  
649 Phytoplankton Growth and Major Nutrient Drawdown in the Southern Ocean." *Nature*  
650 *Communications* 12 (1): 884. <https://doi.org/10.1038/s41467-021-21122-6>.
- 651 Buma, A. GJ, De Baar, H. JW, Nolting, R. F. and A. J. Van Bennekom. 1991. "Metal Enrichment  
652 Experiments in the Weddell-Scotia Seas: Effects of Iron and Manganese on Various Plankton  
653 Communities." *Limnology and Oceanography* 36 (8): 1865–1878.
- 654 Campbell, D., Hurry V., Clarke, A. K., Gustafsson, P. and G. Öquist. 1998. "Chlorophyll  
655 Fluorescence Analysis of Cyanobacterial Photosynthesis and Acclimation." *Microbiology and*  
656 *Molecular Biology Reviews* 62 (3): 667–83. [https://doi.org/10.1128/MMBR.62.3.667-](https://doi.org/10.1128/MMBR.62.3.667-683.1998)  
657 683.1998.
- 658 Cassar, N., Wright, S. W., Thomson, P. G., Trull, T. W., Westwood, K. J., de Salas, M., Davidson, A.,  
659 Pearce, I., Davies, D. M. and R. J. Matear. 2015. "The Relation of Mixed-Layer Net  
660 Community Production to Phytoplankton Community Composition in the Southern Ocean."  
661 *Global Biogeochemical Cycles* 29 (4): 446–62. <https://doi.org/10.1002/2014GB004936>.
- 662 Deppeler, S. L. and A. T. Davidson. 2017. "Southern Ocean Phytoplankton in a Changing Climate."  
663 *Frontiers in Marine Science* 4 (February). <https://doi.org/10.3389/fmars.2017.00040>.
- 664 Ellwood, M. J., Strzepek, R. F., Strutton, P. G., Trull, T. W., Fourquez, M., & Boyd, P. W. (2020).  
665 Distinct iron cycling in a Southern Ocean eddy. *Nature communications*, 11(1), 1-8.
- 666 Eriksen, R., Trull, T. W., Davies, D., Jansen, P., Davidson, A. T., Westwood, K., and R. van den  
667 Enden. 2018. "Seasonal Succession of Phytoplankton Community Structure from  
668 Autonomous Sampling at the Australian Southern Ocean Time Series (SOTS) Observatory."  
669 *Marine Ecology Progress Series* 589 (February): 13–31. <https://doi.org/10.3354/meps12420>.
- 670 Ferreira, F. and N. A. Straus. 1994. "Iron Deprivation in Cyanobacteria." *Journal of Applied*  
671 *Phycology* 6 (2): 199–210. <https://doi.org/10.1007/BF02186073>.

672 Fourquez, M., Bressac, M., Deppeler, S. L., Ellwood, M., Obernosterer, I., Trull, T. W. and P. W.  
673 Boyd. 2020. "Microbial Competition in the Subpolar Southern Ocean: An Fe–C Co-  
674 Limitation Experiment." *Frontiers in Marine Science* 6 (January): 776.  
675 <https://doi.org/10.3389/fmars.2019.00776>.

676 Gao, X., Bowler, C. and E. Kazamia. 2021. "Iron Metabolism Strategies in Diatoms." Edited by  
677 Janneke Balk. *Journal of Experimental Botany* 72 (6): 2165–80.  
678 <https://doi.org/10.1093/jxb/eraa575>.

679 Greene, R. M., Geider, R. J., Kolber, Z. and P. G. Falkowski. 1992. "Iron-Induced Changes in Light  
680 Harvesting and Photochemical Energy Conversion Processes in Eukaryotic Marine Algae."  
681 *Plant Physiology* 100 (2): 565–75. <https://doi.org/10.1104/pp.100.2.565>.

682 Holmes, T. M., Wuttig, K., Chase, Z., Schallenberg, C., van der Merwe, P., Townsend, A. T., &  
683 Bowie, A. R. (2020). Glacial and hydrothermal sources of dissolved iron (II) in Southern  
684 Ocean waters surrounding Heard and McDonald Islands. *Journal of Geophysical Research:*  
685 *Oceans*, 125, e2020JC016286. <https://doi.org/10.1029/2020JC016286>

686 Hopkinson, B. M. and K. A. Barbeau. 2008. "Interactive Influences of Iron and Light Limitation on  
687 Phytoplankton at Subsurface Chlorophyll Maxima in the Eastern North Pacific." *Limnology*  
688 *and Oceanography* 53 (4): 1303–18. <https://doi.org/10.4319/lo.2008.53.4.1303>.

689 Hoppe, C.J.M., Klaas, C., Ossebaar, S., Soppa, M.A., Cheah, W., Laglera, L.M., Santos-Echeandia, J.,  
690 et al. 2017. "Controls of Primary Production in Two Phytoplankton Blooms in the Antarctic  
691 Circumpolar Current." *Deep Sea Research Part II: Topical Studies in Oceanography* 138  
692 (April): 63–73. <https://doi.org/10.1016/j.dsr2.2015.10.005>.

693 Hutchins, D. A., Sedwick, P. N., DiTullio, G. R., Boyd, P. W., Quéguiner, B., Griffiths, F. B. and C.  
694 Crossley. 2001. "Control of Phytoplankton Growth by Iron and Silicic Acid Availability in  
695 the Subantarctic Southern Ocean: Experimental Results from the SAZ Project." *Journal of*  
696 *Geophysical Research: Oceans* 106 (C12): 31559–72. <https://doi.org/10.1029/2000JC000333>.

697 Jackson, G. A. 2005. "Role of Algal Aggregation in Vertical Carbon Export during SOIREE and in  
698 Other Low Biomass Environments." *Geophysical Research Letters* 32 (13): L13607.  
699 <https://doi.org/10.1029/2005GL023180>.

700 Koblížek, M., Kaftan, D. and L. Nedbal. 2001. "On the Relationship between the Non-Photochemical  
701 Quenching of the Chlorophyll Fluorescence and the Photosystem II Light Harvesting  
702 Efficiency. A Repetitive Flash Fluorescence Induction Study," 12.

703 Marie, D., Partensky, F., Vaultot, D. and C. Brussaard. 1999. "Enumeration of Phytoplankton,  
704 Bacteria, and Viruses in Marine Samples." *Current Protocols in Cytometry* 10 (1).  
705 <https://doi.org/10.1002/0471142956.cy1111s10>.

706 Moore, C. M. 2013. "Processes and Patterns of Oceanic Nutrient Limitation." *Nature Geosciences*. 6:  
707 10.

708 Ohnemus, D. C., Krause, J. W., Brzezinski, M. A., Collier, J. L., Baines, S. B. and B. S. Twining.  
709 2018. "The Chemical Form of Silicon in Marine Synechococcus." *Marine Chemistry* 206  
710 (October): 44–51. <https://doi.org/10.1016/j.marchem.2018.08.004>.

711 Paasche, E. 1973. "Silicon and the Ecology of Marine Plankton Diatoms. I. Thalassiosira Pseudonana  
712 (Cyclotella Nana) Grown in a Chemostat with Silicate as Limiting Nutrient." *Marine Biology*  
713 19 (2): 117–26. <https://doi.org/10.1007/BF00353582>.

714 Peers, G. and N. M. Price. 2004. "A Role for Manganese in Superoxide Dismutases and Growth of  
715 Iron-Deficient Diatoms." *Limnology and Oceanography* 49 (5): 1774–83.  
716 <https://doi.org/10.4319/lo.2004.49.5.1774>.

717 Perron, M.G., Proemse, B. C., Strzelec, M., Gault-Ringold, M., Boyd, P. W., Sanz Rodriguez, E.,  
718 Paull, B. and A. R. Bowie. 2020. "Origin, Transport and Deposition of Aerosol Iron to  
719 Australian Coastal Waters." *Atmospheric Environment* 228 (May): 117432.  
720 <https://doi.org/10.1016/j.atmosenv.2020.117432>.

721 Petrou, K., Hassler, C. S., Doblin, M. A., Shelly, K., Schoemann, V., van den Enden, R., Wright, S.  
722 and P. J. Ralph. 2011. "Iron-Limitation and High Light Stress on Phytoplankton Populations  
723 from the Australian Sub-Antarctic Zone (SAZ)." *Deep Sea Research Part II: Topical Studies*  
724 *in Oceanography* 58 (21–22): 2200–2211. <https://doi.org/10.1016/j.dsr2.2011.05.020>.

725 R Core Team (2020). R: A language and environment for statistical computing. R Foundation for  
726 Statistical Computing, Vienna, Austria. URL <https://www.R-project.org/>

- 727 Rees, C., Pender, L., Sherrin, K., Schwanger, C., Hughes, P., Tibben, S., Marouchos, A. and Mark  
728 Rayner. 2018. "Methods for Reproducible Shipboard SFA Nutrient Measurement Using  
729 RMNS and Automated Data Processing." *Limnology and Oceanography: Methods*,  
730 December. <https://doi.org/10.1002/lom3.10294>.
- 731 Rintoul, S. R. and T. W. Trull. 2001a. "Seasonal Evolution of the Mixed Layer in the Subantarctic  
732 Zone South of Australia." *Journal of Geophysical Research: Oceans* 106 (C12): 31447–62.  
733 <https://doi.org/10.1029/2000JC000329>.
- 734 Salomon, E. and N. Keren. 2011. "Manganese Limitation Induces Changes in the Activity and in the  
735 Organization of Photosynthetic Complexes in the Cyanobacterium *Synechocystis* Sp. Strain  
736 PCC 6803." *Plant Physiology* 155 (1): 571–79. <https://doi.org/10.1104/pp.110.164269>.
- 737 Scharek, R., Van Leeuwe, M. A., and H. JW De Baar. 1997. "Responses of Southern Ocean  
738 Phytoplankton to the Addition of Trace Metals." *Deep Sea Research Part II: Topical Studies  
739 in Oceanography* 44 (1–2): 209–227.
- 740 Sedwick, P. N., DiTullio, G. R., Hutchins, D. A., Boyd, P. W., Griffiths, F. B., Crossley, A. C., Trull,  
741 T. W. and B. Quéguiner. 1999. "Limitation of Algal Growth by Iron Deficiency in the  
742 Australian Subantarctic Region." *Geophysical Research Letters* 26 (18): 2865–68.  
743 <https://doi.org/10.1029/1998GL002284>.
- 744 Sedwick, P. N., DiTullio, G. R. and D. J. Mackey. 2000. "Iron and Manganese in the Ross Sea,  
745 Antarctica: Seasonal Iron Limitation in Antarctic Shelf Waters." *Journal of Geophysical  
746 Research: Oceans* 105 (C5): 11321–36. <https://doi.org/10.1029/2000JC000256>.
- 747 Sedwick, P.N., Bowie, A.R. and T.W. Trull. 2008. "Dissolved Iron in the Australian Sector of the  
748 Southern Ocean (CLIVAR SR3 Section): Meridional and Seasonal Trends." *Deep Sea  
749 Research Part I: Oceanographic Research Papers* 55 (8): 911–25.  
750 <https://doi.org/10.1016/j.dsr.2008.03.011>.
- 751 Strzepek, R. F., Maldonado, M. T., Hunter, K. A., Frew, R. D. and P. W. Boyd. 2011. "Adaptive  
752 Strategies by Southern Ocean Phytoplankton to Lessen Iron Limitation: Uptake of  
753 Organically Complexed Iron and Reduced Cellular Iron Requirements." *Limnology and  
754 Oceanography* 56 (6): 1983–2002. <https://doi.org/10.4319/lo.2011.56.6.1983>.
- 755 Suggett, D. J., MacIntyre, H. L. and R. J. Geider. 2004. "Evaluation of Biophysical and Optical  
756 Determinations of Light Absorption by Photosystem II in Phytoplankton: Evaluation of Light  
757 Absorption by PSII." *Limnology and Oceanography: Methods* 2 (10): 316–32.  
758 <https://doi.org/10.4319/lom.2004.2.316>.
- 759 Suggett, D. J., Moore, C. M., Hickman, A. E., and R. J. Geider. 2009. "Interpretation of Fast  
760 Repetition Rate (FRR) Fluorescence: Signatures of Phytoplankton Community Structure  
761 versus Physiological State." *Marine Ecology Progress Series* 376 (February): 1–19.  
762 <https://doi.org/10.3354/meps07830>.
- 763 Sunda, W. G. and S. A. Huntsman. 1995. "Iron Uptake and Growth Limitation in Oceanic and Coastal  
764 Phytoplankton." *Marine Chemistry* 50 (1–4): 189–206. [https://doi.org/10.1016/0304-  
765 4203\(95\)00035-P](https://doi.org/10.1016/0304-4203(95)00035-P).
- 766 Twining, B. S., Baines, S. B. and N. S. Fisher. 2004. "Element Stoichiometries of Individual Plankton  
767 Cells Collected during the Southern Ocean Iron Experiment (SOFeX)." *Limnology and  
768 Oceanography* 49 (6): 2115–28. <https://doi.org/10.4319/lo.2004.49.6.2115>.
- 769 Twining, B. S., Nuñez-Milland, D., Vogt, S., Johnson, R. S. and P. N. Sedwick. 2010. "Variations in  
770 *Synechococcus* Cell Quotas of Phosphorus, Sulfur, Manganese, Iron, Nickel, and Zinc within  
771 Mesoscale Eddies in the Sargasso Sea." *Limnology and Oceanography* 55 (2): 492–506.  
772 <https://doi.org/10.4319/lo.2010.55.2.0492>.
- 773 Waite, A. M., Safi, K. A., Hall, J. A. and S. D. Nodder. 2000. "Mass Sedimentation of Picoplankton  
774 Embedded in Organic Aggregates." *Limnology and Oceanography* 45 (1): 87–97.  
775 <https://doi.org/10.4319/lo.2000.45.1.0087>.
- 776 Westwood, K. J., F. Griffiths, B., Webb, J. P. and S. W. Wright. 2011. "Primary Production in the  
777 Sub-Antarctic and Polar Frontal Zones South of Tasmania, Australia; SAZ-Sense Survey,  
778 2007." *Deep Sea Research Part II: Topical Studies in Oceanography* 58 (21–22): 2162–78.  
779 <https://doi.org/10.1016/j.dsr2.2011.05.017>.

780 Wolfe-Simon, F., Starovoytov, V., Reinfelder, J. R., Schofield, O. and P. G. Falkowski. 2006.  
781 "Localization and Role of Manganese Superoxide Dismutase in a Marine Diatom." *Plant*  
782 *Physiology* 142 (4): 1701–9. <https://doi.org/10.1104/pp.106.088963>.  
783 Wu, M., McCain, J. S. P., Rowland, E., Middag, R., Sandgren, M., Allen, A. E. and E. M. Bertrand.  
784 2019. "Manganese and Iron Deficiency in Southern Ocean Phaeocystis Antarctica  
785 Populations Revealed through Taxon-Specific Protein Indicators." *Nature Communications*  
786 10 (1): 3582. <https://doi.org/10.1038/s41467-019-11426-z>.  
787